Analysis of Noise and Cycle Selection in a Loran Receiver

C.O. Lee Boyce Jr., Sherman C. Lo,
J. David Powell, and Per K. Enge
Stanford University
Stanford, California 94305

Abstract— **Thermal and atmospheric noise distort envelope measurements in a Loran receiver, and may cause the receiver to select the wrong cycle during signal acquisition. A cycle error would persist during signal tracking and result in a ranging error of 3,000 km. The probability of a wrong cycle selection is dependent on the signal-to-noise ratio and on the algorithm used in signal acquisition. In this paper, we develop a mathematical model to predict the probability of wrong cycle selection in a Loran receiver, which uses a ratio test as a cycle selection algorithm, when subjected to Gaussian noise.**

Previous methods of calculating the probability of wrong cycle selection have been based on empirical data from an Austron 5000 Loran receiver. These data are used to produce a Gaussian approximation of envelope-to-cycle delay (ECD) and to derive the probability of wrong cycle selection from excursions of ECD in excess of 5 μs. Through simulation, we show this empirical method provides a conservative over-bound of the probability of wrong cycle selection versus SNR. However, the novel methods developed in the paper show a theoretical bound which is 1 to 4 dB lower.

I. Overview

A Loran receiver derives tower range estimate from the time-of-arrival measurement of an incoming Loran pulse. The receiver bases the arrival measurement on the third positive zero-crossing, or standard zero-crossing (SZC), which occurs 30 μs from the start of the Loran signal. While most methods for determining the SZC are proprietary, Peterson published an algorithm which uses the ratio of two envelope measurements to select the SZC [1].

Atmosphere and thermal noise internal to a receiver can corrupt both envelope measurements and the ratio of these measurements. The receiver's cycle selection algorithm uses the envelope ratio to find the SZC, therefore, distortions of the ratio can cause the receiver to select the wrong cycle at acquisition. For each cycle off from the true SZC, the range error will increase by 3,000 km. Without additional information, such as receiver integrity monitoring, selection of the wrong cycle at acquisition will carry over through signal tracking.

In this paper, we will examine the effect of Gaussian noise on Loran envelope measurements within a receiver and on the ratio of these measurements. Furthermore, we will use the statistics of the ratio calculation to determine the probability of wrong cycle selection, and to develop a mathematical model to predict the probability of wrong zero-crossing, P[Wrong Cycle], or wrong cycle selection, which is more accurate than previous empirical models.

II. Development

A. Receiver Front End

We begin our noise analysis by examining the effect of Gaussian noise on an incoming Loran signal through a typical receiver front end. Fig. 1 shows an example of a Loran front end that has been modeled in Matlab. The first red pulse in the figure is a received Loran pulse exciting the receiver's antenna. Next, the incoming pulse is filtered, sampled, and mixed down to the in-phase (I) and quadrature (Q) components which then forms the complex envelope.

The receiver averages the complex envelope data to reduce the impact of noise on the signal. The act of averaging improves the signal power to noise power ratio or signal-to-noise ratio (SNR). We will define the total SNR as the SNR of the averaged signal.

With the averaged signal, the receiver can estimate the pulse's time-of-arrival. As mentioned in the previous section, the SZC is used as a common reference for the arrival time of the pulse. However, since only the envelope data is available in the receiver and not the raw carrier, the zero crossing is found by a ratio test.

The receiver performs the test by taking the ratio of two sample points 15 μs apart along the envelope. We define this measurement as $\mathrm{Ratio}(\tau)$,

$$\mathrm{Ratio}(\tau) \equiv \mathrm{Envelope}(\tau - 15\,\mathrm{s})/\mathrm{Envelope}(\tau)$$

where $\mathrm{Envelope}(\tau)$ is the Loran envelope amplitude of the τ μs point.

With the mathematical description of the Loran signal given by [2], the receiver can form $\mathrm{Ratio}(\tau)$ along all points of the waveform.

Fig. 2 depicts the envelope in blue and the underlying carrier in red. $\mathrm{Ratio}(\tau)$, shown in green, is seen to be monotonically increasing over the first 50 μs of the pulse. From the model of an ideal Loran pulse, we can calculate $\mathrm{Ratio}(30)$, the envelope ratio at the SZC, to be approximately 0.4.

When trying to find the SZC on a real Loran pulse, the receiver takes the ratio of all envelope values. The sample which forms the envelope ratio that is closest to 0.4 determines the SZC. From the phase of the sample, the receiver can refine its estimate of the SZC. In Fig. 2, the red dot at 30 μs denotes the true SZC, while black x's corresponding zero-crossing that are either early or late and would be considered wrong cycles if selected by the receiver as the SZC..

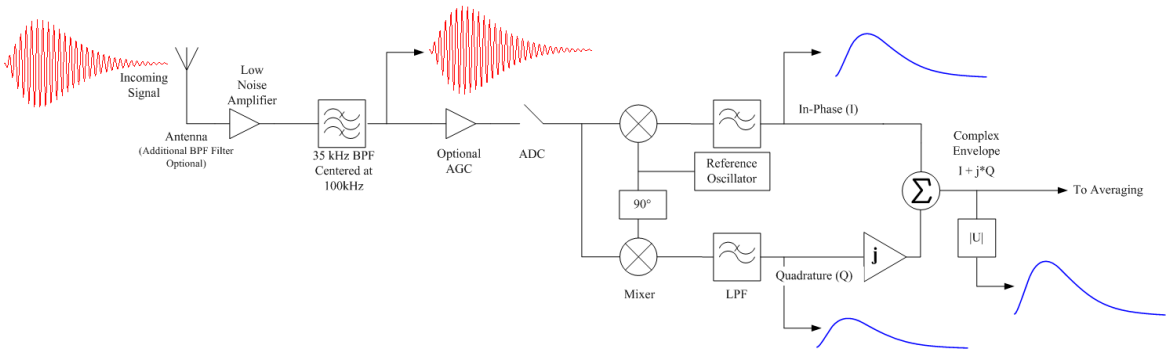

Fig. 1: Diagram of the front end of a Loran receiver.

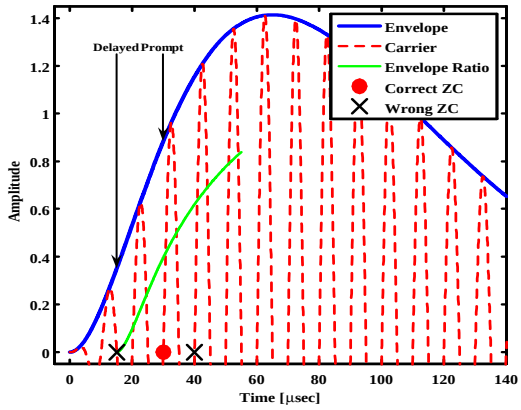

Fig. 2: Loran envelope and ratio test.

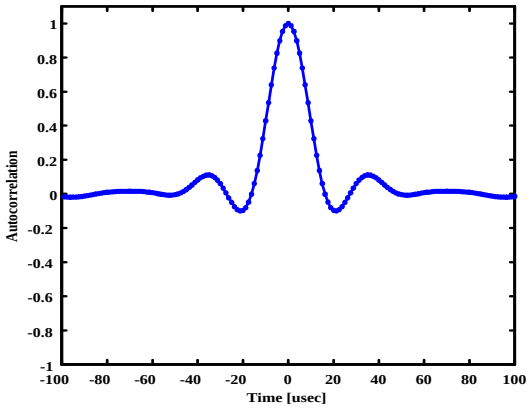

Fig. 3: Autocorrelation of I samples.

This process of determining the SZC from the envelope phase measurements is hampered by noise. Noise can distort the envelope measurement and therefore distort the ratio result. If the ratio is used to determine the zero crossing of the underlying carrier and the noise on the ratio measurement leads the receiver to choose an early or late zero crossing from the SZC, then the range estimate will incur a 3,000 m error.

With an understanding of the algorithm involved in cycle selection, we will now examine the statistics of the I & Q channel noise and the envelope noise. By examining the statistics involved we will develop equations governing the probability of the wrong cycle being chosen for the SZC.

B. I & Q Statistics

The statistics of the I & Q measurements were determined through simulating a known carrier passing through our Loran front end. Since the mixing process requires multiplications and the use of linear filters, we expect the process to be linear, and to preserve the Gaussian nature of the noise. However, the low-pass filtering leads to correlation between samples, depending on the data rate. Fig. 3 shows the autocorrelation of the I channel when sampled at 800 kHz. The samples are almost completely uncorrelated after 60 μs.

Our Loran receiver design produces I & Q samples at 50 kHz, therefore, the period between samples is 20 μs. From the plot, we see that the correlation is small at this time. Hence, to simplify the analysis, we will ignore the correlation, and approximate the noise as independent and identically distributed (IID).

To demonstrate the Gaussian nature of the errors and the validity of the approximation of the noise being IID, Fig. 4 (a) and (b) show the cumulative distribution function (cdf) and 1 minus the cdf of the I channel data errors when sampled at 50 kHz. From the plots, we see the Gaussian approximation fits the data well. The Q channel results were similar. Therefore, we will model both the I & Q errors of our 50 kHz data as IID Gaussian noise.

C. Envelope Statistics

While the I & Q channels are Gaussian in nature, the envelope measurement will not be Gaussian due to the non-linear nature of the magnitude operation. The magnitude of the envelope is made by forming the root-sum-square (RSS) of the I & Q measurements, therefore, the statistics of envelope measurements is dependent on the statistics of both channels,

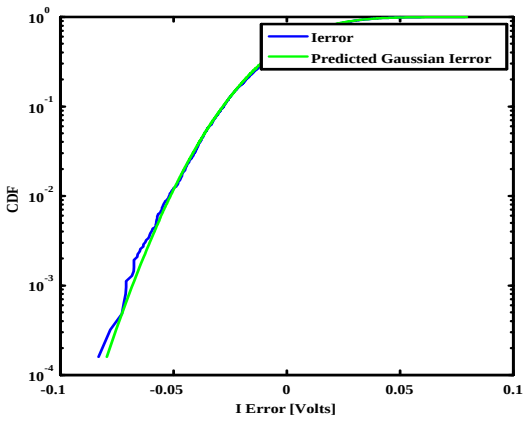

(a) CDF of I Channel Error

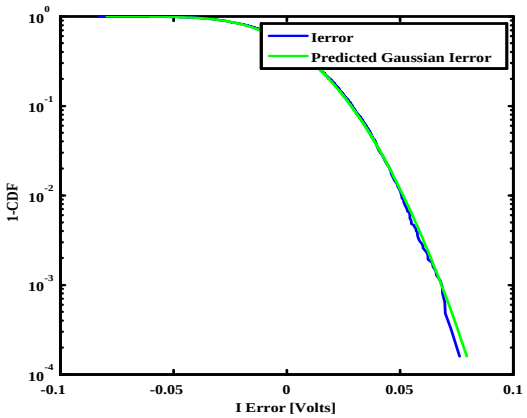

(b) APD of I Channel Error

Fig. 4: Comparison of Gaussian CDF and simulated data for I channel data.

not just the I & Q errors.

Without loss of generality, we can model the incoming signal phasor as lying completely in the I direction with Gaussian noise superimposed on it. We will model the I channel as a Gaussian or normal random variable, $N(\mu, \sigma)$, where μ represents the magnitude of the incoming signal, and σ is the variance of the Gaussian noise. The Q channel may be modeled purely as noise so its statistics are $N(0, \sigma)$. Fig. 5 depicts the vector sum of the true envelope and a given realization of the noise. The shading is the projection of the joint probability distribution function (pdf) underlying the noise.

A Rice distribution results from the root-sum-squaring of two non-zero mean Gaussian variates. Since the envelope measurement is composed of the I & Q measurements, the pdf of the envelope follows a Rice distribution, in general.

The pdf of a Rice distribution, $f_Z(z|\mu, \sigma)$, is given by [3],

$$f_Z(z|\mu,\sigma) = \frac{z}{\sigma^2} \exp\left(-\left(\frac{z^2+\mu^2}{2\sigma^2}\right)\right) I_0\left(\frac{z\mu}{\sigma^2}\right) \quad (1)$$

where $I_0(x)$ is the modified Bessel function of the first kind.

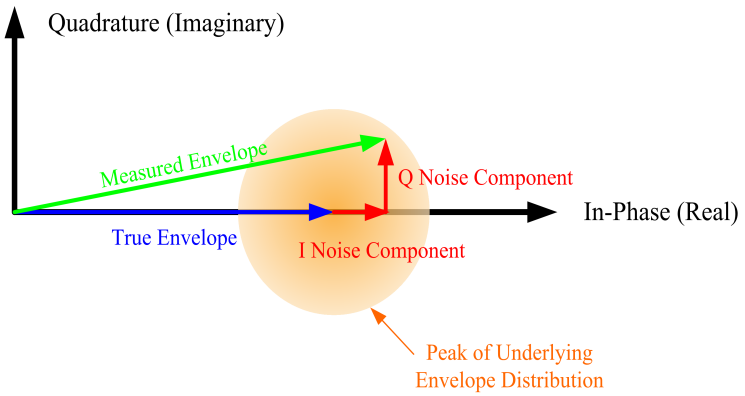

Fig. 5: I-Q plane view of noise added to an envelope voltage.

The SNR of a Loran signal is the ratio of the standard sampling point divided by the root-mean-square (rms) value of the noise and is defined by [2] to be,

$$\begin{aligned} SNR &\equiv \frac{SSP_{rms}}{Noise_{rms}} \\ &= \frac{SSP_{rms}}{\sigma_{Noise}}. \end{aligned} \quad (2)$$

where the SSP is the amplitude of the pulse at 25 μs. If we take μ to be the rms of the SSP, then from Eq. 1 and 2, we see that the envelope distribution is dependent on the SNR.

Fig. 6 (a) through (c) highlight this dependency, through a series of plots of the joint pdf of the I & Q channels for varying cases of SNR. In this series of figures, the joint pdf is shown in orange over a range of values. In Fig. 6 (a), there is no Loran signal present, therefore, the peak of the joint distribution falls at the origin since only the noise accounts for the envelope measurement.

We are interested in determining the envelope pdf, therefore, we would need to integrate the joint pdf over a disk, outlined by a blue circle, and then normalized by the disk's area. Doing so with this joint pdf, we would find the envelope follows a Rayleigh distribution, which is defined as the RSS of two zero-mean Gaussian variates.

As we increase the SNR, we return back to a Rice distribution as shown in Fig. 6 (b), where the SNR is 0 dB. Now, the peak has shifted in the I direction, since, without loss of generality, all of the signal may be taken to be in this direction. Here, the Q component also contributes to the magnitude of the envelope, and so the distribution is best described by a Rice distribution where only one of the Gaussian variates is zero-mean.

As we further increase the SNR, as shown in Fig. 6 (c), we find that the Q component contributes little to the magnitude of the envelope. Instead, Q errors contribute to envelope phase errors. Since only the I component affects the magnitude, then the envelope loses dependence on the Q errors and takes on the identical statistics as the I error, and hence, becomes Gaussian.

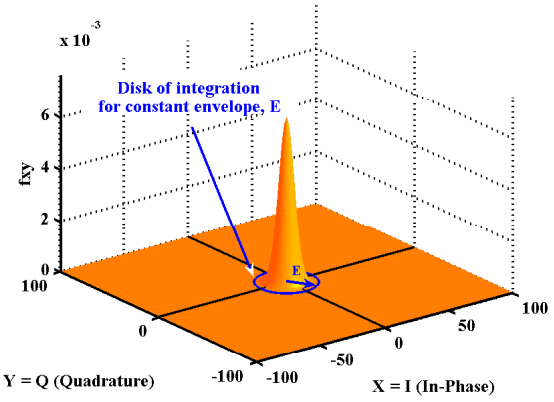

(a) Joint probability distribution of two Gaussian variables with zero-mean and equal variance. Indicative of noise-only case (SNR = $-\infty$ dB).

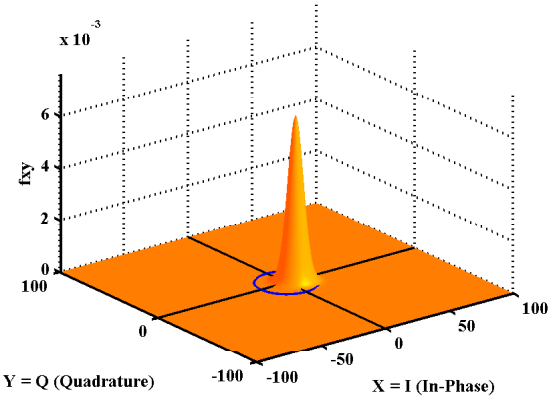

(b) Joint probability distribution of one zero-mean and one finite-mean Gaussian variable with equal variance. Indicative of low SNR case (SNR = 0 dB).

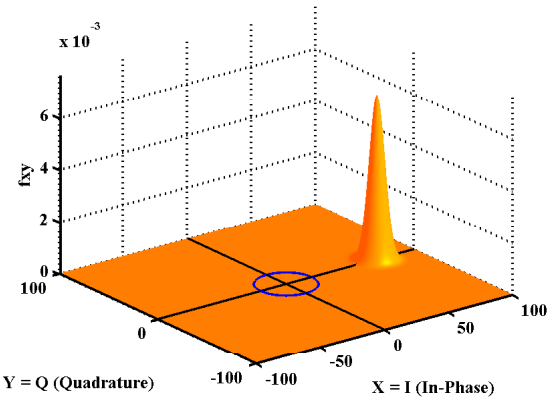

(c) Joint probability distribution of one zero-mean and one finite-mean Gaussian variables with equal variance. Indicative of high SNR case (SNR = 20 dB).

Fig. 6: Joint probability distribution functions for I & Q channel.

Thus, we see the envelope error distribution degenerates from Rician to Rayleigh when the SNR is infinitesimally small and degenerates from Rician to Gaussian when the SNR is greater than 20 dB.

D. Ratio

By using the statistics of the errors on the envelope measurements, we may now proceed to develop the distributions governing the ratio of two envelope measurements. We will then show how these distributions may be used to calculate the probability of wrong cycle selection for the signal's SNR.

Noise will cause Ratio(30) to vary around its ideal value of 0.4. To determine the distribution of the ratio point, from [4], we can calculate the probability density function of the ratio, q, of two variables, z_1 and z_2, by

$$q = \frac{z_2}{z_1}$$

$$f_Q(q) = \int_{x=0}^{\infty} z_1 \; f_{Z_1}(z_1) \; f_{Z_2}(qz_1) \; dz_1 \tag{3}$$

If we take the ratio of two, zero-mean, finite variance Gaussian variables, we form a Cauchy distribution [4]. Since Loran will always be present, to ensure complete generality and exactness, and to cover a variety of SNRs, we will take the ratio of two Rician variates since they account for finite-mean Gaussian variables.

Using two envelope values that follow Rice distributions, we can combine Eqs. 1 and 3 to form the pdf of the envelope ratio, $f_{\mathrm{R}}(q)$, as

$$\begin{aligned} f_{\mathrm{R}}(q) &= \int_{-\infty}^{q} \xi \frac{\xi}{\sigma^2} \exp\left(-\left(\frac{\xi^2+\nu^2}{2\sigma^2}\right)\right) I_0\left(\frac{\xi\nu}{\sigma^2}\right) \frac{q\xi}{\sigma^2} \\ &\quad \times \exp\left(-\left(\frac{q^2\xi^2+\nu^2}{2\sigma^2}\right)\right) I_0\left(\frac{q\xi\nu}{\sigma^2}\right) d\xi \\ &= \int_{-\infty}^{q} \frac{q\xi^3}{\sigma^4} \exp\left(-\left(\frac{\xi^2+q^2\xi^2+2\nu^2}{2\sigma^2}\right)\right) \\ &\quad \times I_0\left(\frac{\xi\nu}{\sigma^2}\right) I_0\left(\frac{q\xi\nu}{\sigma^2}\right) d\xi. \end{aligned} \tag{4}$$

We may now numerically integrate Eq. 4 to form the cdf, thereby determining the probability of achieving a particular ratio value. In practice, we found for SNR $>$ 25 dB, the Gaussian approximation allowed us to get around numerical integration issues, and thus Gaussian distributions were used for higher SNRs.

As an alternate to the analytical calculation, we may attempt to approximate the noise of the ratio as Gaussian. Fig. 7 (a) and (b) show that for high SNR, this Gaussian approximation of the ratio compares well with only a slight offset to the theoretical calculation. However, we find that the approximation performs poorly at low SNR as seen in 8 (a) and (b). For low SNR values, the error lies mainly in the ability for the Gaussian variate to achieve negative values, whereas the envelope measurements are strictly positive. The black dots in the graphs depict sample data numerically generated to confirm the results.

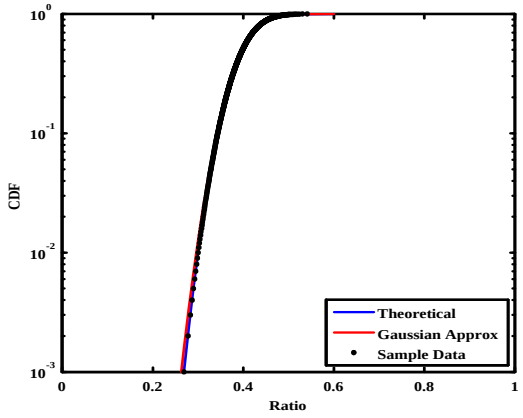

(a) CDF of Ratio(30) for SNR = 20 dB

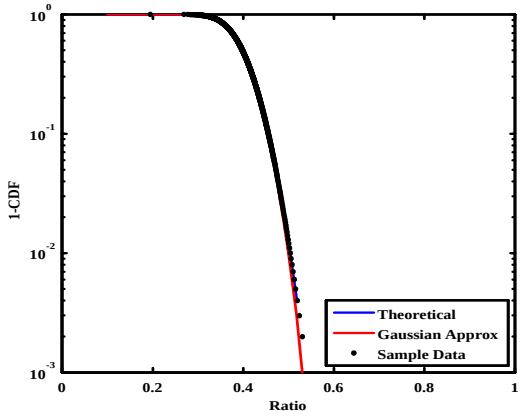

(b) 1-CDF of Ratio(30) for SNR = 20 dB

Fig. 7: Comparison of the Theoretical Calculation, Gaussian Approximation and simulated data for Ratio(30) for SNR = 2.

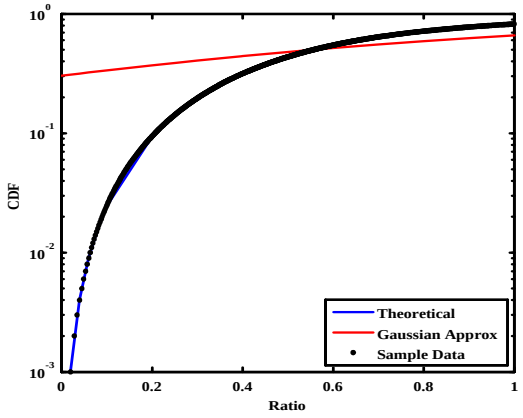

(a) CDF of Ratio(30) for SNR = 0 dB

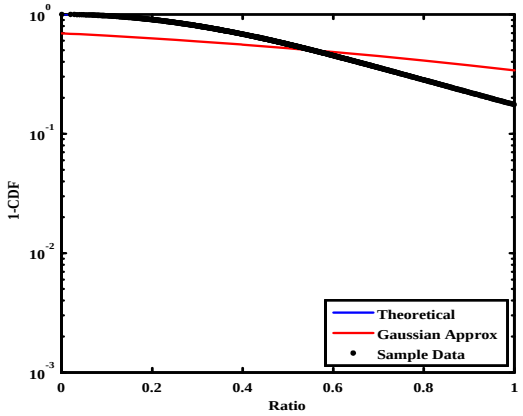

(b) 1-CDF of Ratio(30) for SNR = 0 dB

Fig. 8: Comparison of the Theoretical Calculation, Gaussian Approximation and simulated data for ratio values for high SNR.

With the ideal value and the distribution of Ratio(30), we wish to calculate how far from this ideal would Ratio(30) need to drift before the receiver mistakes it as belonging to the previous or the next Loran cycle. An offset in the time estimate of 5 μs would result in a wrong cycle selection, therefore, we can set bounds on Ratio(30) to lie between Ratio(25) and Ratio(35) in order to obtain the correct cycle. Therefore, a wrong cycle selection will occur if

$$\begin{aligned} \text{Ratio}(30) &\leq \text{Ratio}(25) \text{ or} \\ \text{Ratio}(30) &\geq \text{Ratio}(35) \end{aligned}$$

By using the cdf of Ratio(30) for a given SNR, we can obtain the probability of wrong cycle selection, or P[Wrong Cycle], by summing the probabilities of Ratio(30) meeting the above conditions.

As shown in [5], an alternate method of determining P[Wrong Cycle] uses the empirically derived statistics of the envelope-to-cycle delay (ECD). Based on historical data, the variance of ECD for an Austron 5000 Loran receiver was found to be

$$\sigma_{ECD_{Old}} = 42/\sqrt{N \cdot SNR} \ \mu\text{s} \tag{5}$$

With recent developments in receiver design, Peterson believes this variance may be reduced to be

$$\sigma_{ECD_{New}} = 28/\sqrt{N \cdot SNR} \ \mu\text{s} \tag{6}$$

In a similar manner to the bounding of the Ratio(30) value, should the ECD vary by more than 5 μs, then a cycle slip will occur. Integrating a zero-mean Gaussian distribution with a variance given by Eq. 5 or 6, allows us to determine P[Wrong Cycle] using the "Austron" empirical approximation.

III. Results

Given we have three methods to determine P[Wrong Cycle], we wish to determine the accuracy of their predictions. To do so, we use a software Loran receiver based on [1] and compare the theoretical and empirical performance predictions. Simulated Loran signals of varying amplitudes corrupted by a Gaussian white sequence were fed into the software receiver.

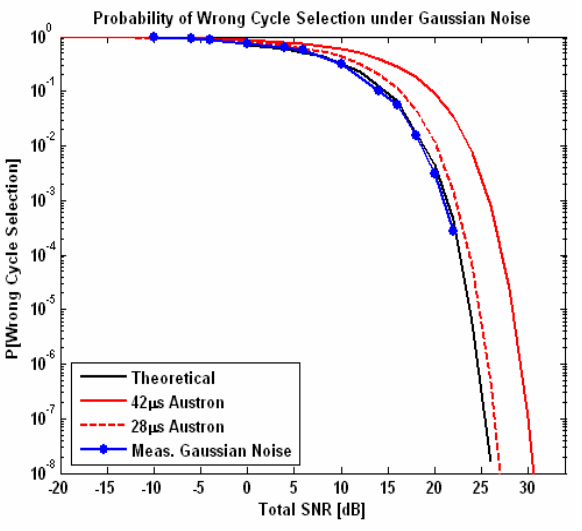

Fig. 9: Probability of wrong cycle selection given the total tower SNR under Gaussian noise.

The receiver, as modeled in Fig. 1, mixed and averaged the signal's complex envelope over a five second interval. By using the ratio method described in Section II-A, the receiver determined the pulses's SZC and estimated its time-of-arrival.

Since we simulated the Loran signals, we know the true TOA. If the receiver's estimated TOA differed from the true TOA by more than 10 μs, the receiver had selected the wrong cycle. By running the acquisition software over long periods of time we could develop the distributions of P[Wrong Cycle] for various SNR.

Fig. 9 compares P[Wrong Cycle] obtained by the three methods: the first, is the theoretical derivation developed in this paper, and the next two use the Austron approximation given by a ECD variances according to Eqs. 5 and 6.

To account for the effects of averaging, the x-axis is given in total SNR which is the SNR multiplied by the number of pulses averaged over the interval. Shown in blue are the results obtained by using a Loran receiver with simulated Loran signals where white Gaussian sequence has been added.

We find that the theoretical predictions match the actual performance of the receiver quite well. We also find that the 28 μs Austron estimate over bounds P[Wrong Cycle] by approximately 1 dB, while the older 42 μs estimate is conservative by about 4 dB.

IV. Conclusion and Future Work

While the previous estimate of the probability of wrong cycle selection within a receiver using the empirically derived data from the Austron receiver, given by Eq. 6, adequately over bounds a receiver's performance, we may tighten the bound by a dB by using the more precise equations developed in this paper. Though the SNR gain is modest, we have progressed the model from one empirically based on the manufacturing of the receiver, to one which is mathematically based on the ratio algorithm used for cycle selection. Transcending from an empirical model to a mathematical one, we improve our confidence in the use of empirical bounds in previous analyses, and we can introduce a limit on Loran performance which was unknown with the empirical data alone.

Furthermore, while this paper analyzes the effect of Gaussian noise on a receiver, it paves the methodology for the determination of Loran performance in the presence of non-Gaussian atmospheric noise. Using Eq. 3, if we can find the distributions of the atmospheric noise that may be sufficiently described to allow for numerical integration, then we can reformulate P[Wrong Cycle] for various non-Gaussian noise conditions.

Another avenue to pursue for future work is refining the wrong cycle selection condition. Rather than measuring when the expected envelope ratio for the SZC falls out of range, it may be more accurate to examine the probabilities of the ratios at the wrong zero-crossings of being closer to the ideal ratio value of 0.4 than the measurement at the SZC. In light of the good correlation of the probability of wrong cycle selection between the initial method and the simulated results, the increase in complexity in this alternate method may not be warranted.

V. Disclaimer

The views expressed herein are those of the primary author and are not to be construed as official or reflecting the views of the U.S. Coast Guard, Federal Aviation Administration, Department of Transportation or Department of Homeland Security.

VI. Acknowledgements

The authors first and foremost acknowledge Mitch Narins (FAA AND 702) for his support of Loran and the development of this work. In addition, we thank Ben Peterson for his insight and helpful suggestions.

References

[1] Benjamin Peterson, "LORAN C H-Field DDC Receiver," United States Coast Guard Academy Department of Engineering, New London, CT, Tech. Rep. Version 011221, 2001.

[2] "Specification of the Transmitted Loran C Signal," U.S. Department of Transportation, United States Coast Guard, Washington, DC, Tech. Rep. COMDTINST M16562.4A, May 1994.

[3] "http://mathworld.wolfram.com/ricedistribution.html," October 2006.

[4] Alberto Leon-Garcia, *Probability and Random Processes for Electrical Engineers 2nd Ed.* Redding, Massachusetts: Addison-Wesley Publishing Company, May 1994.

[5] Benjamin Peterson, et al., "Hazardously Misleading Information Analysis for Loran LNAV," in *2nd International Symposium on Integration of LORAN-C/Eurofix and EGNOS/Galileo*, June 2002.